Original Investigation

Reproducibility of Hyperpolarized ^{129}Xe MRI Ventilation Defect Percent in Severe Asthma to Evaluate Clinical Trial Feasibility

Sarah Svenningsen, PhD, Marrissa McIntosh, BSc, Alexei Ouriadov, PhD, Alexander M Matheson, BSc, Norman B Konyer, BSc, Rachel L Eddy, PhD, David G McCormack, MD, Michael D Noseworthy, PhD, Parameswaran Nair, MD, PhD, Grace Parraga, PhD

Rationale and Objectives: ^{129}Xe MRI has been developed to noninvasively visualize and quantify the functional consequence of airway obstruction in asthma. Its widespread application requires evidence of intersite reproducibility and agreement. Our objective was to evaluate reproducibility and agreement of ^{129}Xe ventilation MRI measurements in severe asthmatics at two sites.

Materials and Methods: In seven adults with severe asthma, ^{129}Xe ventilation MRI was acquired pre- and post-bronchodilator at two geographic sites within 24-hours. ^{129}Xe MRI signal-to-noise ratio (SNR) was calculated and ventilation abnormalities were quantified as the whole-lung and slice-by-slice ventilation defect percent (VDP). Intraclass correlation coefficients (ICC) and Bland-Altman analysis were used to determine intersite ^{129}Xe VDP reproducibility and agreement.

Results: Whole-lung and slice-by-slice ^{129}Xe VDP measured at both sites were correlated and reproducible (pre-bronchodilator: whole-lung ICC = 0.90, $p = 0.005$, slice-by-slice ICC = 0.78, $p < 0.0001$; post-bronchodilator: whole-lung ICC = 0.94, $p < 0.0001$, slice-by-slice ICC = 0.83, $p < 0.0001$) notwithstanding intersite differences in the ^{129}Xe-dose-equivalent-volume (101 ± 15 mL site 1, 49 ± 6 mL site 2, $p < 0.0001$), gas-mixture (^{129}Xe/^{4}He site 1; ^{129}Xe/N_2 site 2) and SNR (40 ± 19 site 1, 23 ± 5 site 2, $p = 0.02$). Qualitative ^{129}Xe gas distribution differences were observed between sites and slice-by-slice ^{129}Xe VDP, but not whole-lung ^{129}Xe VDP, was significantly lower at site 1 (pre-bronchodilator VDP: whole-lung bias = −3%, $p > 0.99$, slice-by-slice bias = −3%, $p = 0.0001$; post-bronchodilator VDP: whole-lung bias = −2%, $p = 0.59$, slice-by-slice-bias = −2%, $p = 0.0003$).

Conclusion: ^{129}Xe MRI VDP at two different sites measured within 24-hours in the same severe asthmatics were correlated. Qualitative and quantitative intersite differences in ^{129}Xe regional gas distribution and VDP point to site-specific variability that may be due to differences in gas-mixture composition or SNR.

Key Words: Xenon-129; MRI; Lung function; Ventilation; Asthma.

Acad Radiol 2020; ■:1–10

From the Firestone Institute for Respiratory Health, St. Joseph's Healthcare Hamilton, Hamilton, Canada (S.S., P.N.); Department of Medicine, McMaster University, 50 Charlton Avenue East, Hamilton, Ontario, Canada L8N 4A6 (S.S., P.N.); Robarts Research Institute, Western University, London, Canada (M.M., A.M.M., R.L.E., G.P.); Department of Medical Biophysics, Western University, London, Canada (M.M., A.M.M., R.L.E., G.P.); Department of Physics and Astronomy, Western University, London, Canada (A.O.); Imaging Research Centre, St. Joseph's Healthcare Hamilton, Hamilton, Canada (N.B.K.); Department of Medicine, Western University, London, Canada (D.G.M., G.P.); Department of Electrical and Computer Engineering, McMaster University, Hamilton, Canada (M.D.N.). Received December 1, 2019; revised April 7, 2020; accepted April 15, 2020. Funding: The study was supported by a Canadian Respiratory Research Network (CRRN) operating grant. S.S. was supported by Canadian Institutes of Health Research (CIHR) Banting and Canadian Respiratory Research Network (CRRN) postdoctoral fellowship awards. R.L.E. was supported by a National Science and Engineering Research Council (NSERC) post-graduate doctoral award. P.N. was supported by the Frederick E. Hargreave Teva Innovation Chair in Airway Diseases. G.P. was supported by the Canada Research Chair Program. Address correspondence to: S.S. e-mail: svennins@mcmaster.ca

https://doi.org/10.1016/j.acra.2020.04.025

Abbreviations: ACQ asthma control questionnaire, **AQLQ** asthma quality of life questionnaire, **DE** dose-equivalent, **ICC** intraclass correlation coefficients, **MRI** magnetic resonance imaging, **SNR** signal-to-noise ratio, **VDP** ventilation defect percent

INTRODUCTION

Inhaled hyperpolarized gas MRI has been developed as a well-tolerated (1–4) imaging method for the noninvasive visualization and quantification of inhaled gas distribution in patients with pulmonary disease. Seminal studies in asthma (5–11), chronic obstructive pulmonary disease (12,13) and cystic fibrosis (14) confirmed the feasibility and clinical relevance of quantitative biomarkers of ventilation derived from hyperpolarized ^{3}He gas MRI, the most established being the ventilation defect percent (VDP). However, in consideration of the global ^{3}He shortage, researchers

recently united and embraced the transition to ^{129}Xe gas to accelerate widespread clinical translation. It is now well-established that ^{129}Xe MRI-based biomarkers of inhaled gas distribution are similar to ^{3}He MRI (15−18), correlate with standard measures of airflow obstruction (15,17,19−24), and are sensitive to subclinical disease (19) and treatment response (16,25). High scan-rescan repeatability of ^{129}Xe VDP at a single site has been reported in healthy volunteers (26), subjects with asthma (21), chronic obstructive pulmonary disease (17), and cystic fibrosis (27). The variability and population heterogeneity of ^{129}Xe VDP in pediatric cystic fibrosis has also been investigated, which recently revealed a similar VDP for two clinically matched cohorts studied at different research sites by two observers (23). The authors also concluded that VDP, measured by two observers, was reproducible and in strong agreement (23). However, intersite reproducibility has not yet been investigated in the same patients who were scanned over a short time period at different research sites.

The direct comparison of ^{129}Xe ventilation MRI measurements across sites is challenging because image acquisition, postprocessing and quantification procedures are not standardized. Acquisition variables including magnetic field strength, scanner vendor, radiofrequency coil hardware, pulse sequence, ^{129}Xe dosing strategies, and administration technique may all affect ventilation measurements and introduce site-specific variability or bias. Postprocessing and ventilation quantification pipelines are also inconsistent (28−33). It is pertinent to understand and consider biases when generalizing ^{129}Xe ventilation data from different sites. Furthermore, intersite standardization and measurement reproducibility will be critical to ascertain if multi-site clinical trials are undertaken for pooled data acquired at different sites.

Following two decades of development and clinical study, quantitative assessment of ventilation by ^{129}Xe MRI is mature and well-established at more than 10 academic institutions across Europe, Canada, and the United States. As such, the infrastructure and rationale for multicenter studies exists, with particular clinical interest in evaluating the efficacy of biologics and other nonpharmacologic interventions for the treatment of severe asthma. To explore the feasibility of multicenter clinical trials, our objective was to prospectively evaluate hyperpolarized ^{129}Xe ventilation MRI reproducibility and agreement in participants with severe asthma at two different research sites (133 km apart), using 3T scanners with similar hardware and software, measured within 24 hours. Our secondary objective was to compare intersite, intraobserver, and interobserver ^{129}Xe VDP reproducibility and agreement. Patients with severe asthma who are often poorly controlled experience highly variable symptoms over short periods of time and hence this evaluation probes physiologic variability, geographic, center-specific, and hardware differences.

MATERIALS AND METHODS

Subjects and Study Design

To prospectively evaluate the two-site reproducibility of ^{129}Xe ventilation MRI, seven adults with a diagnosis of severe asthma (16) underwent spirometry and hyperpolarized ^{129}Xe MRI pre- and post-bronchodilator and completed the Asthma Control Questionnaire and Asthma Quality of Life Questionnaire at two sites within 24 hours: Western University (site 1) in London, Canada and Firestone Institute for Respiratory Health (site 2) in Hamilton, Canada. Site order was randomized. At both sites, pre-bronchodilator spirometry was performed followed by pre-bronchodilator ^{129}Xe MRI, bronchodilator was subsequently inhaled, and after 20 minutes post-bronchodilator ^{129}Xe MRI was performed followed by post-bronchodilator spirometry. All participants were recruited from the Firestone Institute for Respiratory Health and provided written-informed-consent to an ethics-board-approved protocol at site 1 (University of Western Ontario Health Sciences Research Ethics Board) and site 2 (Hamilton Integrated Research Ethics Board).

Spirometry, Bronchodilator Reversibility, and FeNO

Spirometry was performed using a *Platinum Elite Series* plethysmograph (MGC Diagnostics; Medical Graphics Corporation, Saint Paul) at site 1 and a *CPFS/D USB* spirometer (MGC Diagnostics) at site 2. Participants withheld short-acting β-agonists for $\geq$6 hours, long-acting β-agonists for $\geq$12 hours and long-acting muscarinic antagonists for $\geq$24 hours prior to their study visits. For post-bronchodilator measurements, four 100 μg doses of *Novo-Salbutamol HFA* (Teva Novopharm Ltd.; Toronto, Canada) were delivered through a metered dose inhaler using an *AeroChamber Plus* spacer (Trudell Medical International; London, Canada). Fractional exhaled nitric oxide was measured using a *Niox Vero*® (Aerocrine; Solna, Sweden) portable exhaled nitric oxide analyzer at site 2.

Image Acquisition

Pulmonary ^{1}H and hyperpolarized ^{129}Xe MRI were acquired during breath-hold in the coronal plane, pre- and post-bronchodilator, at the two sites using *Discovery MR750* 3.0 Tesla systems (General Electric Health Care; Milwaukee) with similar hardware and software. The same custom-built, unshielded quadrature-asymmetric bird-cage coil, tuned to the resonant frequency of ^{129}Xe, ensuring high level of the B_1 field homogeneity (~11% over entire lung) was used to enable hyperpolarized ^{129}Xe MRI (34). Spin-exchange polarizer systems (Polarean 9820 at site 1; Polarean 9800 at site 2) were used to polarize isotopically enriched ^{129}Xe gas (86%; ~400 mL at site 1; ~500 mL at site 2) that was dispensed into a prefilled mixing syringe (600 mL of ^{4}He at site 1; 500 mL of N_2 at site 2) to achieve a fixed dose of ~1 L

that was transferred to a Tedlar bag (Jensen Inert Products, Coral Springs) for participant delivery. ^{129}Xe polarization was measured at both sites using a polarization measurement station (Polarean Inc., Durham) and the dose-equivalent (DE) volume of 100% enriched, 100% polarized ^{129}Xe was calculated as previously described (35). Following inhalation of the 1 L dose (^{129}Xe/^{4}He mixture at site 1; ^{129}Xe/N_2 mixture at site 2) from functional residual capacity, hyperpolarized ^{129}Xe static-ventilation images were acquired using a coronal plane 3D fast gradient recalled echo sequence (10 seconds data acquisition, TE = 1.5 ms, TR = 5.1 ms, initial flip angle = 1.3°, variable flip angle, receive bandwidth = 16 kHz, field of view = 40 × 40 × 24 cm^3; reconstructed matrix size = 128 × 128 × 16; voxel size = 3 × 3 × 15 mm^3) as previously described (16). A matching pulmonary ^{1}H image was acquired prior to the ^{129}Xe static-ventilation image to delineate the thoracic cavity. As previously described, ^{1}H MRI was acquired following inhalation of 1 L of N_2 gas from functional residual capacity using the MRI whole-body radiofrequency coil and a fast-spoiled gradient-recalled-echo sequence (9 seconds data acquisition, TE = 1.2 ms, TR = 4.3 ms, flip angle = 20°, field of view = 40 × 40 cm; matrix size = 128 × 128; 16 slices; voxel size = 3 × 3 × 15 mm^3) (16).

Image Analysis

The signal-to-noise ratio (SNR) and VDP for ^{129}Xe static-ventilation images acquired at both sites were calculated using the analysis pipelines previously described (15,30). We report both whole-lung and slice-by-slice VDP for ^{129}Xe static ventilation images. All images ($n = 28$), after randomization, were reviewed and quantified by a single observer (S.S.). As previously described, the role of the observer is to place fiducial markers on the ^{1}H and ^{129}Xe MRI datasets to permit landmark-based affine registration, manually remove the trachea from ^{129}Xe MRI and edit the ^{1}H MRI automated segmentation of the thoracic cavity (30). To evaluate intraobserver and interobserver variability of whole-lung ^{129}Xe VDP, pre-bronchodilator images acquired at both sites ($n = 14$) were randomized and quantified by two trained observers (S.S., observer 1 and M.M., observer 2), and measurements were repeated two times each (14 datasets × 2 rounds × 2 observers). S.S. and M.M. have 7 years and 1 year of lung imaging experience, respectively.

Statistical Tests

Data were tested for normality using the Shapiro-Wilk normality test and when data were not normal, nonparametric tests were performed. Paired t tests and Wilcoxon matched-pairs signed rank tests were performed to determine if there were differences in clinical and imaging measurements between the two sites. The difference between repeated forced expiratory volume in 1 second (FEV_1), whole-lung and slice-by-slice ^{129}Xe MRI VDP (pre- and post-bronchodilator at site 1 and 2) was determined using a one-way repeated measures analysis of variance (ANOVA) with Sidak's multiple comparisons test for parametric data or Friedman test with Dunn's multiple comparisons test for nonparametric data. Unadjusted and adjusted p values are reported. Pearson and Spearman correlation coefficients were used to evaluate the relationship between whole-lung and slice-by-slice ^{129}Xe MRI VDP at site 1 and 2. Intraclass correlation coefficients (ICC) and Bland-Altman analysis were used to evaluate intersite, intraobserver, and interobserver whole-lung and slice-by-slice ^{129}Xe VDP reproducibility and agreement. ICC values were calculated based on an absolute-agreement, 2-way mixed-effects model. Statistical analyses were performed using GraphPad Prism 8.00 (La Jolla) and SPSS 23.00 (IBM Corporation, Armonk), and results were considered significant when the probability of making a Type I error was <5% ($p < 0.05$).

RESULTS

Table 1 shows demographics, clinical characteristics, and spirometry measurements for seven severe asthmatics in whom

TABLE 1. Subject Demographics, Clinical Characteristics, and Spirometry

	Severe Asthma ($n = 7$)
Age y	49 ± 13
Female sex *n* (%)	2 (29)
BMI kg/m^2	34 ± 8
ACQ-5 Score	3.2 ± 1.6
AQLQ Score	3.6 ± 1.7
FEV_1 Pre-BD L	2.04 ± 0.61
FEV_1 Post-BD L	2.40 ± 0.81
FVC Pre-BD L	3.24 ± 1.06
FVC Post-BD L	3.53 ± 1.01
FEV_1/FVC Pre-BD %	64 ± 15
FEV_1/FVC Post-BD %	67 ± 13
Reversibility of FEV_1 %*	7 (-9-45)
Reversibility of FVC %*	6 (-9-33)
FeNO ppb*	23 (6–123)
Sputum eosinophil %*	0.5 (0.0–4.8)
Sputum neutrophil %*	62.4 (5.4–96.7)
Asthma Medications	
ICS dose μg/day*	1200 (800–2000)
OCS dose mg/day*	0 (0–60)
OCS dependent n (%)	2 (29)
Monoclonal antibody *n* (%)	4 (57)

ACQ, asthma control questionnaire; AQLQ, asthma quality of life questionnaire; BD, bronchodilator; BMI, body mass index; FeNO, fractional exhaled nitric oxide; FEV_1, forced expiratory volume in 1 second; FVC, forced vital capacity; ICS, inhaled corticosteroid; OCS, oral corticosteroid.

All reported measurements, except FeNO, sputum eosinophil and neutrophil %, were acquired at site 1. Values are mean ± standard deviation except when indicated otherwise.

* Median (range).

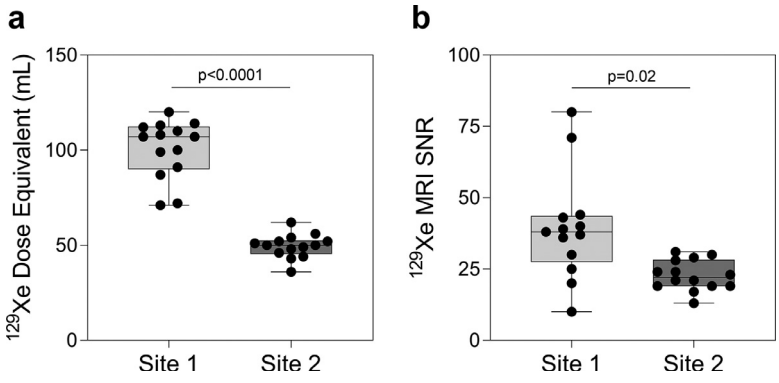

Figure 1. Intersite differences in the dose-equivalent volume of ^{129}Xe administered to the subject and ^{129}Xe MRI SNR.

The dose-equivalent volume of ^{129}Xe administered to the subject (Site 1 = 101 ± 15 mL, Site 2 = 49 ± 6 mL, $p < 0.0001$) (a) and SNR (Site 1 = 40 ± 19, Site 2 = 23 ± 5, $p = 0.02$) (b) were greater at site 1, than at site 2. Box and whisker plots show the minimum, 25th percentile, median, 75th percentile and maximum with individual data points superimposed on the plot. SNR, signal-to-noise ratio.

inhaled gas distribution was evaluated pre- and post-bronchodilator using ^{129}Xe MRI at site 1 and 2. The median (minimum-maximum) time between scanning sessions was 22 (6–28) hours. As shown in Figure 1, the DE volume of ^{129}Xe administered to the subject (101 ± 15 mL at site 1, 49 ± 6 mL at site 2, $p < 0.0001$) and SNR (40 ± 19 at site 1, 23 ± 5 at site 2, $p = 0.02$) were greater at site 1. The total dose-mixture volume administered was not different between sites (1006 ± 18 mL ^{129}Xe/^{4}He mixture at site 1, 1022 ± 36 mL ^{129}Xe/N_2 mixture at site 2, $p = 0.20$). All 28 ^{129}Xe static-ventilation scans (seven pre- and post-bronchodilator at site 1 and 2) were of sufficient quality (based on qualitative inspection) and SNR for VDP quantification.

Representative coronal ^{129}Xe static-ventilation images from three participants, scanned at site 1 and 2, are shown in Figure 2. Focal regions of inhaled gas distribution abnormalities show excellent spatial concordance at both sites. However, intersite differences in gas distribution were also observed such that not all ventilation defects were spatially concordant. For example, for subject 6, a peripheral right lower lobe ventilation defect was observed on the ^{129}Xe static-ventilation image acquired at site 2, but not at site 1 (Fig 2b, white solid-lined box), despite exceptional intersite visual concordance of ventilation distribution in the left upper lobe (Fig 2b, white dash-lined box). For subject 4, a lower left lobe ventilation defect was observed on the ^{129}Xe static-ventilation image acquired at site 1 that corresponded to a hyperventilated (i.e., high signal intensity) region at Site 2.

Figures 3 and 4 quantitatively summarize the intersite reproducibility and agreement of whole-lung ^{129}Xe VDP measured by a single observer. As shown in Figure 3, whole-lung ^{129}Xe VDP from the two sites were not significantly different from one another pre- (11 ± 8% at site 1, 14 ± 11% at site 2; unadjusted $p = 0.68$, adjusted $p > 0.99$) or post-bronchodilator (6 ± 5% at site 1, 8 ± 7% at site 2; unadjusted $p = 0.15$, adjusted $p = 0.59$). The mean post-bronchodilator improvement in whole-lung ^{129}Xe VDP at both sites was similar ($p = 0.75$) (5 ± 4% improvement at site 1; unadjusted $p = 0.003$, adjusted $p = 0.01$; 5 ± 5% improvement at site 2; unadjusted $p = 0.04$, adjusted $p = 0.20$). Whole-lung ^{129}Xe VDP at site 1 and 2 were strongly correlated and reproducible pre- (Fig 4a: r = 0.87, $p = 0.01$; ICC = 0.90, 95% confident interval, 0.48–0.98, $p = 0.005$) and post-bronchodilator (Fig 4c: r = 0.90, $p = 0.02$; ICC = 0.94, 95% confident interval, 0.49–0.99, $p < 0.0001$). Bland-Altman analysis indicated a bias towards smaller whole-lung ^{129}Xe VDP at site 1 as compared to site 2, pre- (Fig 4b: mean bias, −3%; 95% limits of agreement, −14% to 8%) and post-bronchodilator (Fig 4d: mean bias, −2%; 95% limits of agreement, −7% to 2%).

The whole-lung ^{129}Xe VDP analysis reported previously (Fig 3) was repeated to consider the ^{129}Xe MRI VDP of each slice for all subjects (7 subjects, all slices, pre- and postbronchodilator at site 1 and 2). Slice-by-slice ^{129}Xe VDP was significantly lower at site 1 than site 2, both pre- (unadjusted $p < 0.0001$, adjusted $p = 0.0001$) and post-bronchodilator (unadjusted $p < 0.0001$, adjusted $p = 0.0003$). There was a significant improvement post-bronchodilator for slice-by-slice ^{129}Xe VDP at both sites (unadjusted $p = 0.005$, adjusted $p = 0.02$ at site 1; unadjusted $p = 0.003$, adjusted $p = 0.01$ at site 2) that was not significantly different between sites ($p = 0.35$). Slice-by-slice ^{129}Xe VDP at site 1 and 2 were correlated and reproducible pre- (r = 0.74, $p < 0.0001$; ICC = 0.78, 95% confident interval, 0.61–0.87, $p < 0.0001$) and post-bronchodilator (r = 0.72, $p < 0.0001$; ICC = 0.83, 95% confident interval, 0.67–0.90, $p < 0.0001$). Bland-Altman analysis indicated a bias towards lower slice-by-slice ^{129}Xe VDP at site 1 as compared to site 2, pre- (mean bias, −3%; 95% limits of agreement, −16% to 10%) and post-bronchodilator (mean bias, −2%; 95% limits of agreement, −12% to 7%). Table 2 summarizes slice-by-slice ^{129}Xe VDP, comparing pre- and post-bronchodilator VDP at site 1 and site 2, for each subject. Pre-bronchodilator slice-by-slice ^{129}Xe VDP was significantly different between the sites for subjects 6 (unadjusted $p = 0.01$, adjusted $p = 0.04$) and 7 (unadjusted $p < 0.0001$, adjusted $p < 0.0001$). Post-bronchodilator slice-by-slice ^{129}Xe VDP was significantly different between the sites for subjects 2 (unadjusted $p = 0.003$, adjusted $p = 0.01$) and 7 (unadjusted $p = 0.0006$, adjusted $p = 0.002$). In all but one of these cases (subject 6, prebronchodilator), slice-by-slice ^{129}Xe VDP was significantly lower at site 1.

Spirometry was also repeated at both sites. Pre-bronchodilator FEV_1 (2.04 ± 0.61 L at site 1, 1.90 ± 0.57 L at site 2; unadjusted $p = 0.11$, adjusted $p = 0.36$)

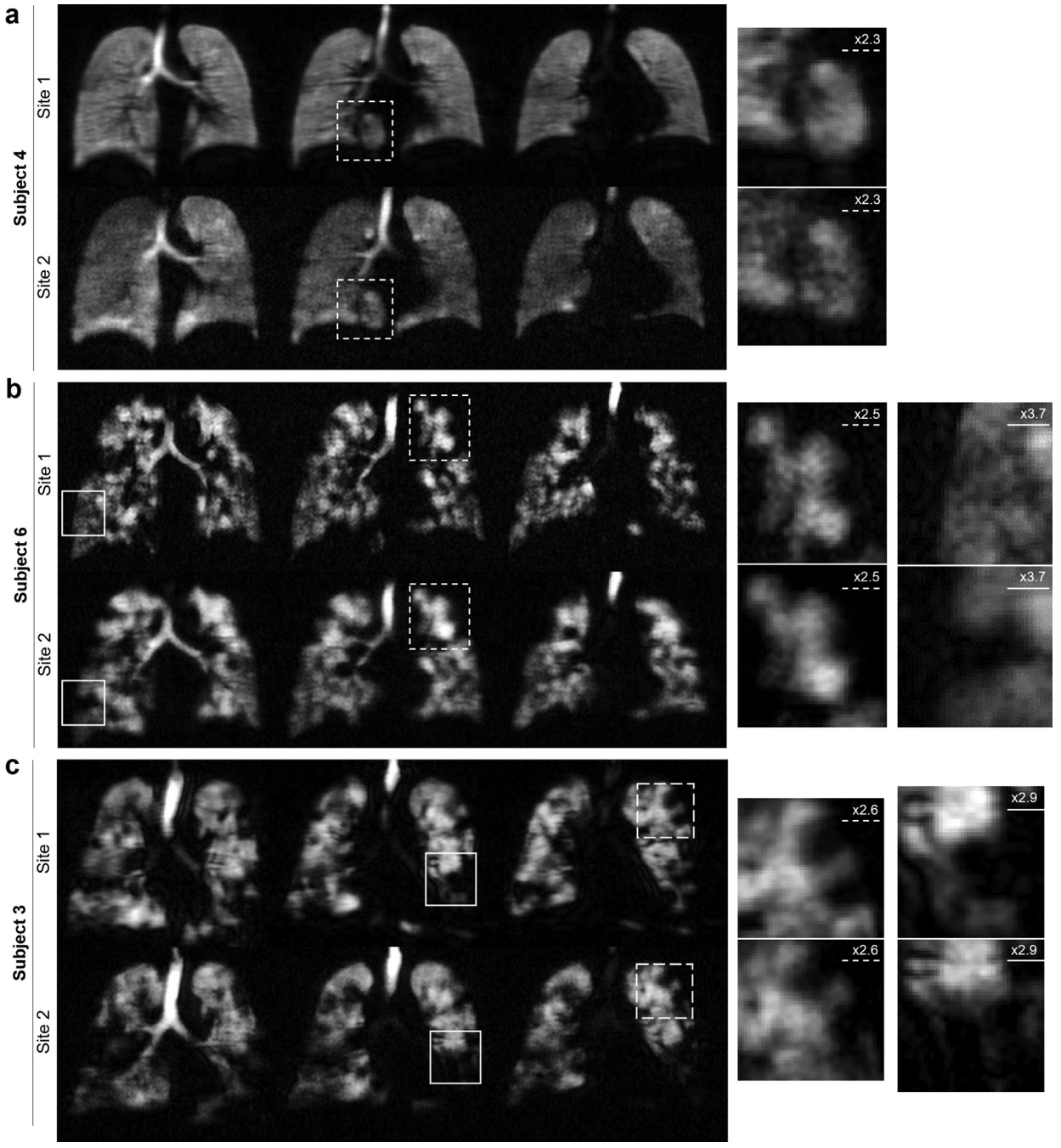

Figure 2. Comparison of ^{129}Xe static-ventilation MRI acquired at site 1 and 2 for representative severe asthmatics.

Anatomically matched coronal ^{129}Xe static-ventilation slices, acquired at site 1 and 2, are shown for three representative subjects with severe asthma. Panels on the right feature regions where the distribution of ^{129}Xe gas was spatial concordant (white dashed line) and discordant (white solid line) between sites. (a) Subject 4: 43-year-old female (post-bronchodilator), 2% VDP at site 1 (DE = 107 mL; SNR = 80), 3% VDP at site 2 (DE = 50 mL; SNR = 19), 2.11 L FEV_1 at site 1, 2.10 L FEV_1 at site 2. (b) Subject 6: 46-year-old male (pre-bronchodilator), 13% VDP at site 1 (DE = 91 mL; SNR = 20), 9% VDP at site 2 (DE = 44 mL; SNR = 30), 2.29 L FEV_1 at site 1, 2.02 L FEV_1 at site 2. (c) 3: 56-year-old male (pre-bronchodilator), 24% VDP at site 1 (DE = 114 mL; SNR = 43), 34% VDP at site 2 (DE = 54 mL; SNR = 28), 1.11 L FEV_1 at site 1, 1.03 L FEV_1 at site 2. DE, dose-equivalent; FEV_1, forced expiratory volume in one second; SNR, signal-to-noise ratio; VDP, ventilation defect percent.

and postbronchodilator FEV_1 (2.40 ± 0.81 L at site 1, 2.29 ± 0.76 L at site 2; unadjusted $p = 0.03$, adjusted $p = 0.10$) were not significantly different between sites. However, in three participants, the intersite difference in FEV_1 was greater than the minimal clinically important difference (≥200 mL (36)) pre-bronchodilator (S2, S6, S7) and in one participant post-bronchodilator (S6). Intersite differences in whole-lung ^{129}Xe VDP were not related to intersite differences in FEV_1 (pre-bronchodilator: r = −0.30, $p = 0.52$; post-bronchodilator: r = −0.43,

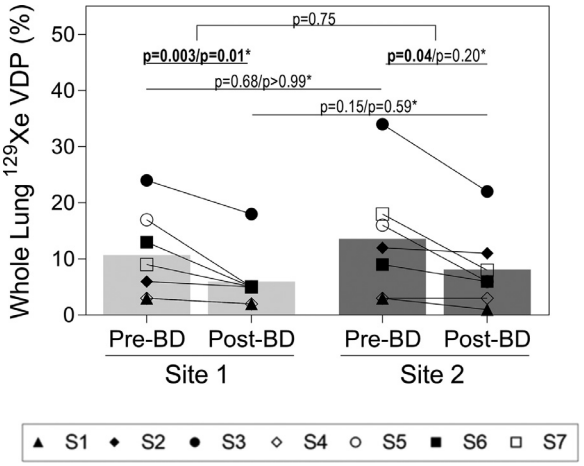

Figure 3. Pre- and post-bronchodilator whole-lung ^{129}Xe MRI ventilation defect percent at site 1 and 2. Whole-lung ^{129}Xe MRI ventilation defect percent (VDP) from the two sites were not significantly different from one another pre- (site 1 = 11 ± 8%, site 2 = 14 ± 11%, $p = 0.68/>0.99$) or post-bronchodilator (site 1 = 6 ± 5%, site 2 = 8 ± 7%, $p = 0.15/0.59$). ^{129}Xe MRI VDP improved post-bronchodilator at both sites (Site 1 mean of difference=−5 ± 4%, $p = 0.003/0.01$; site 2 mean of difference = −5 ± 5%, $p = 0.04/0.20$). The bronchodilator response was not different between sites ($p = 0.75$). Bars show mean with individual values for all subjects superimposed on the plot. Significance of difference between whole-lung ^{129}Xe VDP (pre- and post-bronchodilator at site 1 and 2) was determined using a Friedman test with Dunn's multiple comparisons test (unadjusted and/or adjusted p values*). Bold p values denote statistical significance ($p < 0.05$). BD, bronchodilator; VDP, ventilation defect percent.

$p = 0.33$), ^{129}Xe DE volume (pre-bronchodilator: r = 0.42, $p = 0.35$; post-bronchodilator: r = 0.32, $p = 0.49$) or SNR (pre-bronchodilator: r = −0.29, $p = 0.58$; post-bronchodilator: r = 0.02, $p = 0.97$). The mean improvement in FEV_1 at both sites was similar (363 ± 394 mL or 17 ± 20% improvement at site 1; unadjusted $p = 0.05$, adjusted $p = 0.19$; 384 ± 376 mL or 20 ± 24% improvement at site 2; unadjusted $p = 0.04$, adjusted $p = 0.13$) and strongly correlated (r = 0.90, $p = 0.006$). There were no intersite differences in the time between bronchodilator inhalation and post-bronchodilator ^{129}Xe MRI (23 ± 11 minutes at site 1, 23 ± 8 minutes at site 2, $p = 0.73$), the time between bronchodilator inhalation and post-bronchodilator spirometry (48 ± 16 minutes at site 1, 38 ± 9 minutes at site 2, $p = 0.43$), or the time between post-bronchodilator ^{129}Xe MRI and post-bronchodilator spirometry (25 ± 18 minutes at site 1, 12 ± 4 minutes at site 2, $p = 0.12$).

Table 3 summarizes the intraobserver and interobserver reproducibility and agreement of whole-lung ^{129}Xe VDP measured by two observers. Whole-lung ^{129}Xe VDP was not significantly different between observers and there was high interobserver reproducibility and agreement (round 1, site 1: bias = 0(-4-3)%; ICC = 0.97, $p < 0.0001$; round 1, site 2: bias = 0(-1-1)%; ICC = 0.96, $p < 0.0001$). Similarly, for both observers, whole-lung ^{129}Xe VDP was not significantly different between rounds and there was high intraobserver reproducibility and agreement (observer 1, site 1: bias = 0(-3-2)%; ICC = 0.99, $p < 0.0001$; observer 2, site 1: bias = 0(-1-1)%; ICC = 0.99, $p < 0.0001$). The intersite whole-lung ^{129}Xe VDP bias for both observers were not significantly different from the interobserver bias (observer 1: $p = 0.20$; observer 2: $p = 0.58$) or intraobserver bias (observer 1: $p = 0.09$; observer 2: $p = 0.86$).

DISCUSSION

To better understand hyperpolarized ^{129}Xe ventilation MRI intersite reproducibility, we acquired ^{129}Xe MRI in the same seven participants with severe asthma at two different sites within 24 hours. Research sites with hyperpolarized ^{129}Xe facilities utilize a variety of magnetic field strengths (1.5 T and 3 T), scanner vendors (GE, Siemens, and Philips) and coil configurations (flexible, birdcage, and saddle). Considering hardware differences, and the geographical proximity of ^{129}Xe facilities, the sites included in this reproducibility trial offered a hardware-controlled site-to-site comparison, using MRI systems with similar hardware and software (3T Discovery MR750) and the same birdcage ^{129}Xe coil such that identical pulse sequences could be executed. It is however important to consider that the type of dilution gas (^{4}He at site 1, N_2 at site 2), volume of ^{129}Xe (406 mL at site 1, 522 mL at site 2), DE volume of ^{129}Xe (101 mL at site 1, 49 at site 2), and SNR (40 at site 1, 23 at site 2) were different between sites, which likely impacted inhaled gas distribution and quantification of ventilation defects. Ventilation abnormalities visualized using ^{129}Xe MRI at both sites were quantified as the VDP, using the same semiautomated segmentation software with high intra- and interobserver reproducibility. We reported that whole-lung and slice-by-slice ^{129}Xe VDP quantified from the two sites were strongly correlated and reproducible, and that the post-bronchodilator VDP improvement was not significantly different in a small group of participants. There were however qualitative ^{129}Xe gas distribution differences between sites, and a bias towards lower ^{129}Xe MRI VDP at site 1 compared to site 2, that may have been due to intersite differences in gas-mixture composition or SNR.

The strong correlation and reproducibility of ^{129}Xe VDP quantified at two sites was, to our knowledge, a first demonstration of intersite comparison of hyperpolarized ^{129}Xe MRI. With a similar objective, Couch et al (23) retrospectively compared ^{129}Xe VDP in clinically matched pediatric cystic fibrosis participants studied at two institutions. Similar VDP was reported for both cohorts, despite site-specific differences in MRI hardware (magnetic field strength, scanner vendor, radiofrequency coil) and ^{129}Xe dosing strategies (23). In this previous work, ^{129}Xe VDP was quantified by two observers using a mean-anchored linear binning technique (31). In agreement with our report, interobserver reproducibility of ^{129}Xe VDP was high. The potential for bias imposed by variable postprocessing and ventilation quantification pipelines was recently explored by He et al (37). The

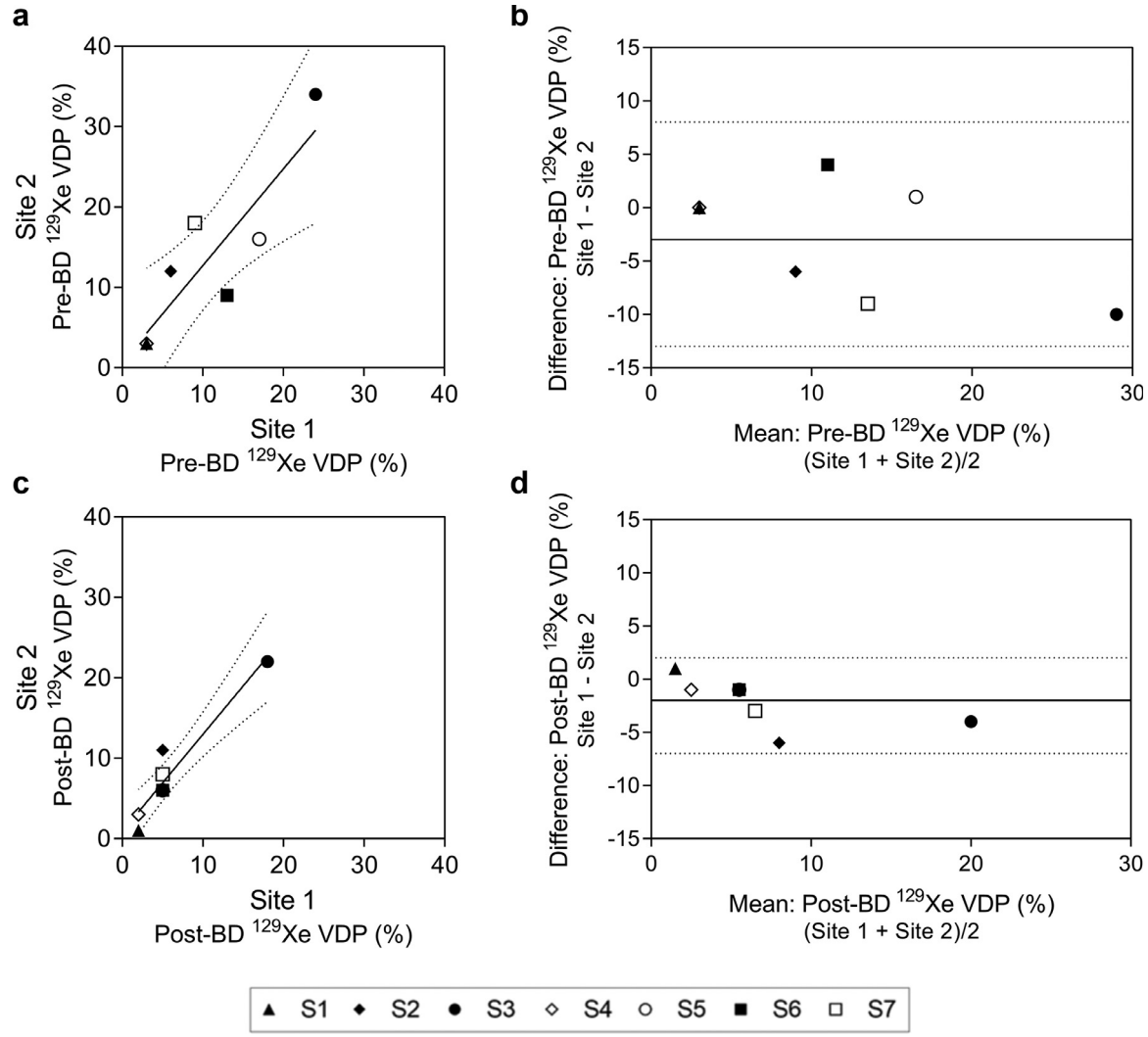

Figure 4. Intersite reproducibility of whole-lung ^{129}Xe MRI ventilation defect percent. (a) Relationship between pre-bronchodilator whole-lung ^{129}Xe VDP at site 1 and 2 ($r = 0.87$, $r^2 = 0.77$, $p = 0.01$, $y = 1.2x + 0.70$). Dotted lines represent the 95% confidence intervals of the regression line. (b) Bland-Altman plot of the difference between pre-bronchodilator whole-lung ^{129}Xe VDP at site 1 and site 2. Plot shows the mean of the paired differences (solid line) and the 95% limits of agreement (dotted lines). Bias= −3% (95% limits of agreement, −14% to 8%).

(c) Relationship between post-bronchodilator whole-lung ^{129}Xe VDP at site 1 and 2 ($r = 0.90$, $r^2 = 0.91$, $p = 0.02$, $y = 1.2x + 0.91$). Dotted lines represent the 95% confidence intervals of the regression line. (d) Bland-Altman plot of the difference between post-bronchodilator whole-lung ^{129}Xe VDP at site 1 and site 2. Plot shows the mean of the paired differences (solid line) and the 95% limits of agreement (dotted lines). Bias = −2% (95% limits of agreement, −7% to 2%). VDP, ventilation defect percent.

comparison of adaptive k-means and linear-binning classification approaches to quantify VDP revealed a modest bias, and that both methods were exceptionally tolerant to poor SNR conditions (37). Our observations, together with those of Couch (31) and He (37), suggest that ^{129}Xe measurements of abnormal ventilation are robust to site-specific differences in MRI acquisition and quantification protocols.

It is important to acknowledge that we observed a bias (smaller ^{129}Xe VDP at site 1 than at site 2 (3% pre-bronchodilator and 2% post-bronchodilator)) that, while not different from the intra- and interobserver differences, was driven by three participants (S2, S3, S7) in whom ^{129}Xe VDP was more than 5% lower at site 1 than at site 2. Based on the ^{3}He MRI literature (38), this difference is likely clinically relevant. Furthermore, it is important to highlight that focal qualitative intersite differences in ^{129}Xe gas distribution were observed in a subset of subjects (Fig 2, white solid line). Considering the intersite differences in FEV_1 (which may be due to differences in spirometry equipment or technician coaching between sites), and the substantial difference in ^{129}Xe polarization, gas mixture composition and SNR between sites, it is difficult to definitively conclude the cause of these differences without further study evaluating the effect of dose mixture composition and DE volume of ^{129}Xe administered to the subject on VDP. We do however speculate that site-specific dose mixture differences may explain the small bias that we observed. Relative to the dose mixture used at site 1 (406 ± 18 mL ^{129}Xe/600 ± 0 mL ^{4}He), the dose mixture at site 2

TABLE 2. Slice-by-Slice Comparison of Pre- and Post-bronchodilator ^{129}Xe MRI Ventilation Defect Percent at Site 1 and 2 for Each Subject

	Site 1 VDP (±SD)			Site 2 VDP (±SD)			Site 1 vs. Site 2 VDP	
Subject	Pre-BD	Post-BD	*p* Value*	Pre-BD	Post-BD	*p* Value*	Pre-BD *p* Value*	Post-BD *p* Value*
1	3 ± 2	2 ± 1	0.37/>0.99	2 ± 1	1 ± 0	**0.02**/0.10	0.73/>0.99	0.08/0.33
2	5 ± 3	5 ± 3	0.67/>0.99	11 ± 5	10 ± 4	0.93/>0.99	**0.02**/0.06	**0.003/0.01**
3	26 ± 11	21 ± 10	0.10/0.40	35 ± 12	27 ± 17	**0.01/0.04**	**0.02**/0.06	0.12/0.48
4	2 ± 2	2 ± 3	0.73/>0.99	3 ± 4	2 ± 2	0.39/>0.99	0.51/>0.99	0.26/>0.99
5	14 ± 10	4 ± 1	**0.003/0.01**	15 ± 4	5 ± 3	**0.002/0.007**	0.44/>0.99	0.54/>0.99
6	13 ± 3	5 ± 3	<**0.0001**/<**0.0001**	8 ± 3	6 ± 2	**0.04**/0.14	**0.01/0.04**	0.30/0.76
7	8 ± 3	4 ± 1	**0.02**/0.09	18 ± 3	9 ± 2	**0.0002/0.0007**	<**0.0001**/<**0.0001**	**0.0006/0.002**

BD, bronchodilator; VDP, ventilation defect percent.

Values are mean ± standard deviation of ^{129}Xe MRI VDP for all slices.

Significance of difference between groups determined using a one-way repeated measures ANOVA with Sidak's multiple comparisons test for parametric data or Friedman test with Dunn's multiple comparisons test for nonparametric data.

* unadjusted/adjusted *p* values. Bold *p* values denote statistical significance ($p < 0.05$).

consisted of a greater volume of hyperpolarized ^{129}Xe gas that was mixed with N_2 (522 ± 36 mL ^{129}Xe/500 ± 0 mL N_2), which has a higher density (1.10 1kg/m^3 for N_2 vs. 0.157 kg/m^3 for ^{4}He) and lower diffusion coefficient (0.216 cm^2/s for N_2 vs. 1.77 cm^2/s for ^{4}He) than ^{4}He. The use of different mixing gases between sites (^{4}He at site 1, N_2 site 2) was based on institutional priorities and decision-making related to a number of factors including cost, ease of inhalation, sensitivity to pathology and desire to mimic the physical properties of air (diffusivity, density, and viscosity). At Site 2, a higher volume of ^{129}Xe gas was used to compensate for the lower ^{129}Xe polarization achieved using the Polarean 9800 hyperpolarizer. Although the difference in dose composition is a limitation of our reproducibility study design, we believe it is highly relevant as dose composition is variable between ^{129}Xe MRI research sites. For example, Ebner et al reported using 0.5−1.0 L volumes of hyperpolarized ^{129}Xe gas diluted to 1.0 L with N_2 gas (39). Consistent with site 2, Walkup et al reported using 0.5 L of hyperpolarized ^{129}Xe gas diluted to 1.0 L with N_2 gas (40). Other studies report using 1.0 L of undiluted hyperpolarized ^{129}Xe gas (41,42). In this study, we hypothesize that the dose mixture used at site 1 may allow gas access to slower filling lung units during the 10 seconds breath-hold required for image acquisition. The white solid lined box in Figure 2b illustrates this concept, showing a ventilation defect observed at site 2, which was hypointense at site 1. Scan-rescan studies at a single site, using volume matched doses of different mixing gases (i.e., ^{4}He and N_2), are necessary to confirm this hypothesis. It is also conceivable that the lower SNR at site 2 may have contributed to this trend. However, our data do not support this notion as inter-site differences in SNR and VDP were not correlated. Regardless of the origin of qualitative and quantitative inter-site differences in ^{129}Xe regional gas distribution and VDP, standardization of acquisition protocols and procedures is encouraged to minimize the potential for site-specific biases.

We also observed a similar improvement in ^{129}Xe VDP following bronchodilator inhalation at both sites. This improvement was expected and is in accordance with a previous study in mild asthma (16). It should be noted that the

TABLE 3. Interobserver and Intraobserved Reproducibility and Agreement of Pre-bronchodilator Whole-Lung ^{129}Xe MRI Ventilation Defect Percent

	VDP (±SD)			Bias* (95%LA)	ICC (95%CI, *p*)
Interobserver:	Observer 1	Observer 2	*p*		
Round 1, Site 1	9 ± 7	9 ± 8	0.70	0 (-4-3)	0.97 (0.85−1.00), $p < 0.0001$
Round 1, Site 2	11 ± 8	11 ± 9	0.60	0 (-1-1)	0.96 (0.80−0.99), $p < 0.0001$
Round 2, Site 1	9 ± 7	9 ± 7	0.67	0 (-5-4)	1.00 (0.98−1.00), $p < 0.0001$
Round 2, Site 2	11 ± 8	11 ± 8	0.89	0 (-4-4)	0.97 (0.81−0.99), $p < 0.0001$
Intraobserver:	*Round 1*	*Round 2*	*p*		
Observer 1, Site 1	9 ± 7	9 ± 7	0.57	0 (-3-2)	0.99 (0.93−1.00), $p < 0.0001$
Observer 1, Site 2	11 ± 8	11 ± 8	0.57	0 (-3-2)	0.99 (0.94−1.00), $p < 0.0001$
Observer 2, Site 1	9 ± 8	9 ± 7	0.36	0 (-1-1)	0.99 (0.99−1.00), $p < 0.0001$
Observer 2, Site 2	11 ± 9	11 ± 8	>0.99	0 (-4-4)	0.98 (0.89−1.00), $p < 0.0001$

CI, confidence interval; ICC, intraclass correlation coefficients; LA, limits of agreement; VDP, ventilation defect percent.

* Bland-Altman bias.

post-bronchodilator improvement in FEV_1, which is considered the gold standard measure of airflow obstruction, was not statistically significant at site 1 or 2 following correction for multiple comparisons. Although not statistically significant, the improvement in FEV_1 was greater than the established cut-off for a clinically relevant improvement (>200 mL and 12%). The difference in treatment effect measured by FEV_1 and ^{129}Xe VDP is of high interest, and may indicate that ^{129}Xe VDP is more sensitive to treatment than FEV_1. If this is in fact true, fewer subjects may be required in drug trials in which ^{129}Xe VDP is the endpoint. Although airway inflammation is known to contribute to ventilation defects visualized by MRI (7), we did not evaluate the effect of anti-inflammatory treatment on ^{129}Xe VDP.

A number of limitations should be considered when interpreting this study. Most importantly, we acknowledge that this work was limited by the small number of subjects. Additionally, qualitative assessment of matched datasets from site 1 and 2 revealed differences in patient positioning and slice location between sites, such that slices were not anatomically matched between sites for some subjects. As a result, we did not quantitatively evaluate the spatial agreement of ventilation and ventilation defect regions between sites, which is highly dependent on accurate registration. There were also potential contributors to site-specific variability that we did not, or could not, control for: (1) changes in airway pathophysiology for participants in the 24-hour period between site acquisitions, (2) site-specific gas mixture and SNR differences, and (3) dose administration technique. The added value of hyperpolarized ^{129}Xe MRI is likely to be clinically relevant in severe asthmatics. Therefore, we elected to evaluate the two-site reproducibility of ^{129}Xe ventilation in a representative cohort of asthmatics who would be considered for multicenter trials of severe asthma therapeutics. As asthma is characterized by variable airflow obstruction, it is possible that there may have been changes in disease pathophysiology between imaging sessions at the two sites; which could have been exacerbated by withdrawal of β-agonists and muscarinic antagonists. Consequently, there is the potential that the time between scans also played a role. Considering the geographical proximity of the sites (133 km) and logistical burden imposed on the study subjects, it was not feasible to reduce the time between scanning sessions. Thus, it may be important to evaluate age-matched healthy controls and an additional cohort of asthmatics with mild, well-controlled disease in future studies. We speculate that similar, or greater, agreement would be observed in mild asthmatics with more stable airflow obstruction and/or chronic obstructive pulmonary disease with more chronic, persistent airflow obstruction. Another limitation is that this study design did not include an intrasite scan-rescan repeatability assessment. This was justified by the high single-site repeatability of ^{129}Xe VDP in asthma reported by Ebner et al (21). Finally, we did not consider intersite differences in B_1^+ homogeneity (nor did we perform inhomogeneity corrections), B_0 field homogeneity or background noise. The relatively short TE used in this work likely minimized the influence of any differences in magnetic field homogeneity between two sites. Furthermore, a multi-site ^{129}Xe phantom study conducted at both sites, utilized the same custom-built, unshielded quadrature-asymmetric bird-cage coil, and confirmed differences in background noise between the sites was negligible (43).

In conclusion, hyperpolarized ^{129}Xe MRI VDP, measured in seven severe asthmatics at two-sites within 24-hours, was reproducible and strongly correlated, while detecting post-bronchodilator responses that were not different. These favorable observations are pertinent as we consider ^{129}Xe VDP as an additional outcome measure to evaluate severe asthma therapeutics in future multicenter clinical trials. Qualitative and quantitative intersite differences in ^{129}Xe regional gas distribution and VDP point to site-specific variability. Factors effecting inhaled gas distribution and quantitative outcome measures are poorly understood and warrant further study. To enable comparable ^{129}Xe ventilation measurements across sites a significant collaborative effort is required to standardize dose composition, dose volume, dose delivery, image acquisition, and quantitative analysis protocols. Fortunately, an international consortium has been established to spearhead these initiatives and disseminate standardized protocols. As the field embarks on regulatory approvals and multicenter trials the pertinence of these efforts has been recognized and are now underway.

ACKNOWLEDGMENTS

The authors thank L. Reid-Jones, D. Knipping, M. Kjarsgaard, and C. Huang for helping with the recruitment and assessment of study subjects, and D. Reese, J. Lecomte, C. Awde, and T. DiLeonardo, the MRI technologists who performed the scanning.

REFERENCES

1. Walkup LL, Thomen RP, Akinyi TG, et al. Feasibility, tolerability and safety of pediatric hyperpolarized (129)Xe magnetic resonance imaging in healthy volunteers and children with cystic fibrosis. Pediatr Radiol 2016; 46:1651–1662.
2. Driehuys B, Martinez-Jimenez S, Cleveland ZI, et al. Chronic obstructive pulmonary disease: safety and tolerability of hyperpolarized 129Xe MR imaging in healthy volunteers and patients. Radiology 2012; 262:279–289.
3. Shukla Y, Wheatley A, Kirby M, et al. Hyperpolarized 129Xe magnetic resonance imaging: tolerability in healthy volunteers and subjects with pulmonary disease. Acad Radiol 2012; 19:941–951.
4. Lutey BA, Lefrak SS, Woods JC, et al. Hyperpolarized 3He MR imaging: physiologic monitoring observations and safety considerations in 100 consecutive subjects. Radiology 2008; 248:655–661.
5. Mummy DG, Kruger SJ, Zha W, et al. Ventilation defect percent in helium-3 magnetic resonance imaging as a biomarker of severe outcomes in asthma. J Allergy Clin Immunol 2018; 141:1140–1141. e1144.
6. Thomen RP, Sheshadri A, Quirk JD, et al. Regional ventilation changes in severe asthma after bronchial thermoplasty with (3)He MR imaging and CT. Radiology 2015; 274:250–259.
7. Svenningsen S, Eddy RL, Lim HF, et al. Sputum eosinophilia and magnetic resonance imaging ventilation heterogeneity in severe asthma. Am J Respir Crit Care Med 2018; 197:876–884.

8. Costella S, Kirby M, Maksym GN, et al. Regional pulmonary response to a methacholine challenge using hyperpolarized (3)He magnetic resonance imaging. Respirology 2012; 17:1237–1246.
9. Altes TA, Powers PL, Knight-Scott J, et al. Hyperpolarized 3He MR lung ventilation imaging in asthmatics: preliminary findings. J Magn Reson Imaging 2001; 13:378–384.
10. Svenningsen S, Kirby M, Starr D, et al. What are ventilation defects in asthma? Thorax 2014; 69:63–71.
11. de Lange EE, Altes TA, Patrie JT, et al. Evaluation of asthma with hyperpolarized helium-3 MRI: correlation with clinical severity and spirometry. Chest 2006; 130:1055–1062.
12. Kirby M, Pike D, Coxson HO, et al. Hyperpolarized (3)He ventilation defects used to predict pulmonary exacerbations in mild to moderate chronic obstructive pulmonary disease. Radiology 2014; 273:887–896.
13. Kirby M, Mathew L, Heydarian M, et al. Chronic obstructive pulmonary disease: quantification of bronchodilator effects by using hyperpolarized (3)He MR imaging. Radiology 2011; 261:283–292.
14. Altes TA, Johnson M, Fidler M, et al. Use of hyperpolarized helium-3 MRI to assess response to ivacaftor treatment in patients with cystic fibrosis. J Cyst Fibros 2017; 16:267–274.
15. Kirby M, Svenningsen S, Owrangi A, et al. Hyperpolarized 3He and 129Xe MR imaging in healthy volunteers and patients with chronic obstructive pulmonary disease. Radiology 2012; 265:600–610.
16. Svenningsen S, Kirby M, Starr D, et al. Hyperpolarized (3) He and (129) Xe MRI: differences in asthma before bronchodilation. J Magn Reson Imaging 2013; 38:1521–1530.
17. Stewart NJ, Chan HF, Hughes PJC, et al. Comparison of (3) He and (129) Xe MRI for evaluation of lung microstructure and ventilation at 1.5T. J Magn Reson Imaging 2018; 48:632–642.
18. Tahir BA, Hughes PJC, Robinson SD, et al. Spatial comparison of CT-based surrogates of lung ventilation with hyperpolarized helium-3 and xenon-129 gas MRI in patients undergoing radiation therapy. Int J Radiat Oncol Biol Phys 2018; 102:1276–1286.
19. Walkup LL, Myers K, El-Bietar J, et al. Xenon-129 MRI detects ventilation deficits in paediatric stem cell transplant patients unable to perform spirometry. Eur Respir J 2019; 52:1801779.
20. Virgincar RS, Cleveland ZI, Kaushik SS, et al. Quantitative analysis of hyperpolarized 129Xe ventilation imaging in healthy volunteers and subjects with chronic obstructive pulmonary disease. NMR Biomed 2013; 26:424–435.
21. Ebner L, He M, Virgincar RS, et al. Hyperpolarized 129xenon magnetic resonance imaging to quantify regional ventilation differences in mild to moderate asthma: a prospective comparison between semiautomated ventilation defect percentage calculation and pulmonary function tests. Invest Radiol 2017; 52:120–127.
22. Kanhere N, Couch MJ, Kowalik K, et al. Correlation of lung clearance index with hyperpolarized (129)Xe magnetic resonance imaging in pediatric subjects with cystic fibrosis. Am J Respir Crit Care Med 2017; 196:1073–1075.
23. Couch MJ, Thomen R, Kanhere N, et al. A two-center analysis of hyperpolarized (129)Xe lung MRI in stable pediatric cystic fibrosis: potential as a biomarker for multi-site trials. J Cyst Fibros 2019; 18:728–733.
24. Doganay O, Matin T, Chen M, et al. Time-series hyperpolarized xenon-129 MRI of lobar lung ventilation of COPD in comparison to V/Q-SPECT/CT and CT. Eur Radiol 2018; 29:4058–4067.
25. Rayment JH, Couch MJ, McDonald N, et al. Hyperpolarised (129)Xe magnetic resonance imaging to monitor treatment response in children with cystic fibrosis. Eur Respir J 2019; 53:1802188.
26. Hughes PJC, Smith L, Chan HF, et al. Assessment of the influence of lung inflation state on the quantitative parameters derived from hyperpolarized gas lung ventilation MRI in healthy volunteers. J Appl Physiol (1985) 2019; 126:183–192.
27. Santyr G, Kanhere N, Morgado F, et al. Hyperpolarized gas magnetic resonance imaging of pediatric cystic fibrosis lung disease. Acad Radiol 2019; 26:344–354.
28. He M, Kaushik SS, Robertson SH, et al. Extending semiautomatic ventilation defect analysis for hyperpolarized (129)Xe ventilation MRI. Acad Radiol 2014; 21:1530–1541.
29. Hughes PJC, Horn FC, Collier GJ, et al. Spatial fuzzy c-means thresholding for semiautomated calculation of percentage lung ventilated volume from hyperpolarized gas and (1) H MRI. J Magn Reson Imaging 2018; 47:640–646.
30. Kirby M, Heydarian M, Svenningsen S, et al. Hyperpolarized 3He magnetic resonance functional imaging semiautomated segmentation. Acad Radiol 2012; 19:141–152.
31. Thomen RP, Walkup LL, Roach DJ, et al. Hyperpolarized (129)Xe for investigation of mild cystic fibrosis lung disease in pediatric patients. J Cyst Fibros 2017; 16:275–282.
32. Zha W, Kruger SJ, Cadman RV, et al. Regional heterogeneity of lobar ventilation in asthma using hyperpolarized helium-3 MRI. Acad Radiol 2018; 25:169–178.
33. Tustison NJ, Avants BB, Flors L, et al. Ventilation-based segmentation of the lungs using hyperpolarized (3)He MRI. J Magn Reson Imaging 2011; 34:831–841.
34. Farag A, Wang J, Ouriadov A, et al. Unshielded and asymmetric RF transmit coil for hyperpolarized 129Xe human lung imaging at 3.0 T 2012; Proc Intl Soc Mag Reson Med 20 (2012) abstract #1361.
35. He M, Robertson SH, Kaushik SS, et al. Dose and pulse sequence considerations for hyperpolarized (129)Xe ventilation MRI. Magn Reson Imaging 2015; 33:877–885.
36. Santanello NC, Zhang J, Seidenberg B, et al. What are minimal important changes for asthma measures in a clinical trial? Eur Respir J 1999; 14:23–27.
37. He M, Zha W, Tan F, et al. A comparison of two hyperpolarized (129)Xe MRI ventilation quantification pipelines: the effect of signal to noise ratio. Acad Radiol 2019; 26:949–959.
38. Eddy RL, Svenningsen S, McCormack DG, et al. What is the minimal clinically important difference for helium-3 magnetic resonance imaging ventilation defects? Eur Respir J 2018; 53:1800324.
39. Ebner L, Virgincar RS, He M, et al. Multireader determination of clinically significant obstruction using hyperpolarized (129)Xe-ventilation MRI. AJR Am J Roentgenol 2019; 212:758–765.
40. Walkup LL, Roach DJ, Hall CS, et al. Cyst ventilation heterogeneity and alveolar airspace dilation as early disease markers in lymphangioleiomyomatosis. Ann Am Thorac Soc 2019; 16:1008–1016.
41. Matin TN, Rahman N, Nickol AH, et al. Chronic obstructive pulmonary disease: lobar analysis with hyperpolarized (129)Xe MR imaging. Radiology 2017; 282:857–868.
42. Willmering MM, Niedbalski PJ, Wang H, et al. Improved pulmonary (129) Xe ventilation imaging via 3D-spiral UTE MRI. Magn Reson Med 2020; 84:312–320.
43. Bier EA, Nouls JC, Wang Z, et al. A thermally polarized (129) Xe phantom for quality assurance in multi-center hyperpolarized gas MRI studies. Magn Reson Med 2019; 82:1961–1968.